

Crystal Structure of Hemoprotein Domain of P450BM-3, a Prototype for Microsomal P450's

Kurumbail G. Ravichandran, Sekhar S. Boddupalli, Charles A. Hasemann, Julian A. Peterson, Johann Deisenhofer*

Cytochrome P450BM-3, a bacterial fatty acid monooxygenase, resembles the eukaryotic microsomal P450's and their flavoprotein reductase in primary structure and function. The three-dimensional structure of the hemoprotein domain of P450BM-3 was determined by x-ray diffraction and refined to an *R* factor of 16.9 percent at 2.0 angstrom resolution. The structure consists of an α and a β domain. The active site heme is accessible through a long hydrophobic channel formed primarily by the β domain and the B' and F helices of the α domain. The two molecules in the asymmetric unit differ in conformation around the substrate binding pocket. Substantial differences between P450BM-3 and P450cam, the only other P450 structure available, are observed around the substrate binding pocket and the regions important for redox partner binding. A general mechanism for proton transfer in P450's is also proposed.

Cytochromes P450 are heme-thiolate enzymes that catalyze oxidations of a vast array of hydrophobic compounds of endogenous or environmental origin (1). Of the P450 genes that belong to 36 different families, more than 200 have been identified (2). The primary chemical reaction catalyzed by these monooxygenases is the two-electron activation of molecular oxygen, whereby one atom of dioxygen is inserted into the substrate and, at the same time, the other is reduced to water (3). The cytochromes P450 can be divided into two classes, depending on the nature of the redox partner. Class I P450's are found in the mitochondrial membranes of eukaryotes and in most bacteria and require a flavin adenine dinucleotide (FAD) containing reductase and an iron-sulfur protein; class II P450's are bound to the endoplasmic reticulum and interact directly with a reductase containing FAD and flavin mononucleotide (FMN).

Despite the isolation of many P450's, only one atomic structure is available; P450cam is a 5-exo-hydroxylase of camphor from *Pseudomonas putida* and is a member of class I (4, 5). Crystal structures of P450cam (4, 6) have provided guidelines for understanding the stereospecificity of the hydroxylation reaction, changes in redox poten-

tial, and spin equilibria on substrate binding. However, the lack of definitive amino acid sequence similarity between P450cam and eukaryotic P450's limits its usefulness as a general model for all P450's (7).

The only well-characterized bacterial P450 that belongs to class II is P450BM-3

from *Bacillus megaterium*; P450BM-3 is catalytically self-sufficient in the monooxygenation of fatty acids (8). The holoenzyme [molecular weight (M_r) 119,000], after limited proteolysis with trypsin in the presence of substrate, is cleaved into (i) the NH₂-terminal P450 domain (M_r 55,000), which binds the substrate, and (ii) the COOH-terminal reductase domain (M_r 66,000), which contains FAD and FMN (9). The coding regions for these domains have been genetically engineered and expressed as individual enzymes (10, 11); the activity of the holoenzyme was reconstituted with the recombinant P450 and reductase domains (11).

The functional similarity of P450BM-3 to the eukaryotic class II enzymes is also reflected in their amino acid sequences. The reductase domain of P450BM-3 and microsomal NADPH:P450 reductases (NADPH, nicotinamide adenine dinucleotide phosphate reduced) are about 35 percent identical (12). Similarly, the heme domain shows about 25 to 30 percent sequence identity to the microsomal fatty acid ω -hydroxylases and the *n*-alkane-inducible cytochromes P450 from eukaryotes (13). In contrast, P450BM-3 has only marginal primary structure homology (15 to 20 percent) with P450's from other bacteria and segregates with the eukaryotic families 4 and 52

Table 1. Crystallographic data statistics. The uranyl acetate and the gadolinium chloride derivatives were prepared by soaking native crystals in mother liquor (0.1 M Pipes buffer, pH 6.8, 18 percent PEG 8000, 40 mM MgSO₄, and 15 mM DTT) containing the specified heavy atom reagents at 4°C. The mercury derivative was prepared in the absence of DTT. Heavy atoms were located by isomorphous and anomalous difference Patterson maps and cross-difference Fourier maps. Handedness was determined by including the anomalous signals.

Parameters	Native	Thimerosal	Uranyl acetate		Gadolinium chloride
			I	II	
Soaking concentration (mM)		5.0	1.5	1.0	1.0
Soaking time (days)		2	10	6	2
Data resolution (Å)	2.0	3.5	3.0	3.5	3.5
Data completeness [$I > 2\sigma(I)$] (percent)	73.6	97.0	97.1	96.6	68.6
Data completeness near resolution limit [$I > 2\sigma(I)$] (percent)	45.0	95.7	68.9	95.1	62.6
Measurements [$I > 2\sigma(I)$] (<i>N</i>)	251913	47366	57768	50271	21097
Unique reflections [$I > 2\sigma(I)$]	55129	13579	19362	13517	9599
<i>R</i> _{merge} (percent)*	5.8	3.0	6.3	4.4	3.0
$ \Delta F / F $ †		0.18	0.19	0.11	0.14
<i>R</i> _{cutlis} (percent)‡		0.91	0.73	0.84	0.83
Sites (<i>N</i>)		3	3	1	2
rms $ F_{hkl} /\text{residual}$ §		0.75	1.39	1.03	0.73
Figure of merit	0.57				

* $R_{\text{merge}} = \sum |I_i - \langle I \rangle| / \sum I_i \times 100$ where I_i is the intensity of an individual measurement, and $\langle I \rangle$ is the mean intensity of that reflection. † $|\Delta F|/|F|$ represents the relative isomorphous difference between the native and the derivative structure factor amplitudes and is calculated using the expression $\sum (|F_{\text{P450}}| - |F_{\text{P450}}|) / \sum |F_{\text{P450}}|$ where $|F_{\text{P450}}|$ and $|F_{\text{P450}}|$ refer to the measured structure factor amplitudes of the native and the derivative. ‡ $R_{\text{cutlis}} = \sum (|F_{\text{P450}}| - (|F_{\text{P450}}| - |F_{\text{P450}}|)) / \sum |F_{\text{P450}}|$ where $|F_{\text{P450}}|$ represents the calculated heavy atom structure factor contribution. The summation is valid only for centric reflections. §rms $|F_{\text{P450}}|/\text{residual}$ represents the phasing power of a derivative and is the ratio of the amplitude of the rms heavy atom scattering factor to the rms lack of closure.

K. G. Ravichandran and C. A. Hasemann are with the Howard Hughes Medical Institute, University of Texas Southwestern Medical Center at Dallas, 5323 Harry Hines Boulevard, Dallas, Texas 75235-9050. S. S. Boddupalli and J. A. Peterson are in the Department of Biochemistry, University of Texas Southwestern Medical Center at Dallas. J. Deisenhofer is with the Howard Hughes Medical Institute and the Department of Biochemistry, University of Texas Southwestern Medical Center at Dallas.

*To whom correspondence should be addressed.

in the P450 phylogenetic tree (2). We now describe the crystal structure of the hemo-protein domain of P450BM-3.

Structure determination. Crystals of the hemoprotein domain of P450BM-3 have the symmetry of space group $P2_1$ with unit

cell dimensions $a = 59.4 \text{ \AA}$, $b = 154.0 \text{ \AA}$, $c = 62.2 \text{ \AA}$, and $\beta = 94.7^\circ$, and have two molecules in the asymmetric unit (14). Diffraction data were collected on multi-wire area detectors (Xuong-Hamlin design) coupled to a Rigaku (RU-200) rotating anode generator. The structure was solved by multiple isomorphous replacement (MIR) with four heavy atom derivatives (Table 1). The electron density map calculated with MIR phases to 3.5 \AA resolution and improved by solvent flattening was used for initial tracing of the polypeptide chain, and a $C\alpha$ model was built for ~ 75 percent of the residues; the graphics programs FRODO and O were used for model building (15, 16). A Patterson function based on the Bijvoet differences of the native data independently confirmed the iron positions. The noncrystallographic transformation that relates the two molecules in the asymmetric unit was determined by real space search methods (17). The MIR phases were improved by density averaging with the program DEMON (18). The model was rebuilt in the improved map, and the process of density averaging and refitting of the model was repeated six times to build more than 90 percent of the polypeptide. The model was refined by means of the program X-PLOR (19), with noncrystallographic symmetry restraints. The model was finally refined by simulated annealing without noncrystallographic restraints. At present, the R value is 16.9 percent for all data with

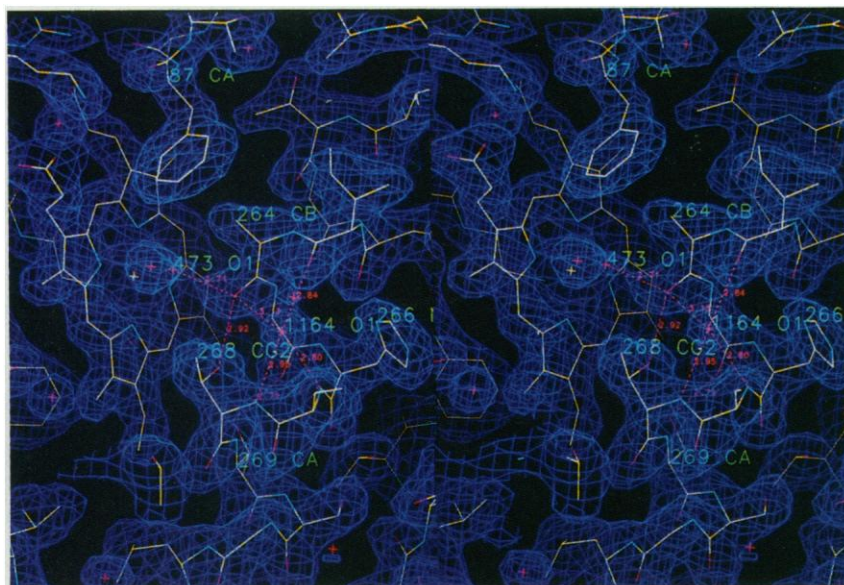


Fig. 1. Stereo view of the final electron density map near the heme. The map was calculated from reflections in the resolution range 20.0 to 2.0 \AA with $(|2F_o| - |F_c|)$ amplitudes and model phases and is contoured at 1σ , where σ is the standard deviation of the electron density map. The current refined model is superimposed and colored by element (oxygen, red; nitrogen, blue; carbon, yellow; sulfur, green; and iron, white). The view is from the distal side of the heme, the proposed direction of substrate entry into the active site. Proximal refers to the face of the heme toward the conserved Cys⁴⁰⁰. The heme and the distorted central part of the I helix are displayed. Hydrogen bonds are inferred from the distance ($< 3.5 \text{ \AA}$) between donor and acceptor; selected hydrogen bonds, with distances in angstroms, are shown as dashed lines.

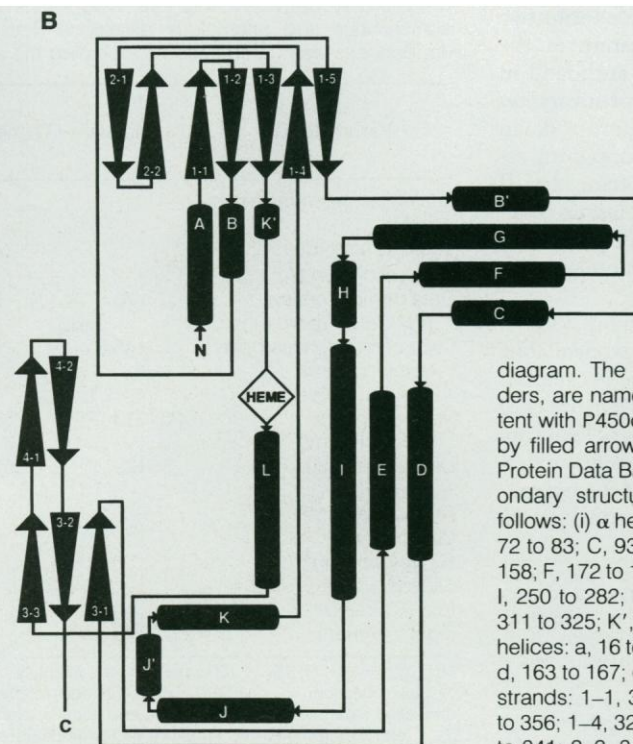
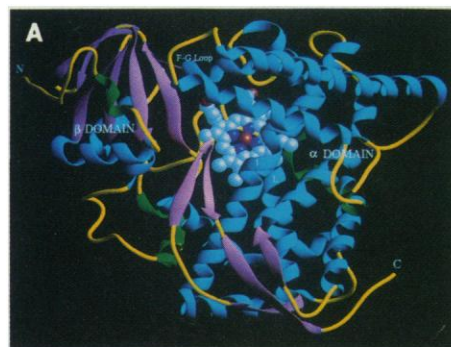


Fig. 2. Polypeptide chain folding and secondary structure of P450BM-3. The NH_2 - and $COOH$ -termini are labeled N and C. **(A)** Ribbon diagram displaying the overall folding of the protein. The α helices are shown in cyan, β strands in magenta, 3_{10} helices in green, and random coil in yellow. **(B)** Topology diagram. The α helices, represented by cylinders, are named in alphabetical order, consistent with P450cam. The β strands, represented by filled arrows, are named according to the Protein Data Bank convention. The various secondary structural elements are assigned as follows: (i) α helices: A, 25 to 37; B, 54 to 62; B', 72 to 83; C, 93 to 104; D, 114 to 132; E, 142 to 158; F, 172 to 189; G, 197 to 226; H, 233 to 239; I, 250 to 282; J, 283 to 298; J', 304 to 310; K, 311 to 325; K', 357 to 361; L, 402 to 419. (ii) 3_{10} helices: a, 16 to 20; b, 105 to 108; c, 109 to 113; d, 163 to 167; e, 375 to 379; f, 381 to 385. (iii) β strands: 1-1, 38 to 44; 1-2, 47 to 53; 1-3, 350 to 356; 1-4, 329 to 335; 1-5, 66 to 70; 2-1, 337 to 341; 2-2, 344 to 348; 3-1, 138 to 141; 3-2, 444 to 451; 3-3, 420 to 424; 4-1, 432 to 436; 4-2, 438 to 442.

$|F_{\text{obs}}| > 2 \sigma(|F_{\text{obs}}|)$ between 20.0 and 2.0 Å resolution (Fig. 1). The root-mean-square (rms) deviation of the bond lengths and bond angles from standard values is 0.016 Å and 3.1°, respectively. The mean coordinate error is estimated to be 0.22 Å based on a Luzzati plot (20) and 0.27 Å based on the SIGMAA method (21).

The model we describe consists of 7895 atoms including 455 solvent molecules. It includes residues 1 to 457 and the heme for both molecules in the asymmetric unit. The 14 residues at the COOH-terminus could not be traced for either molecule. While the overall *B* factor for the entire asymmetric unit is 25 Å², that for the loop between the F and G helices is more than 80 Å² for both molecules, indicating its flexibility.

The molecule has a triangular prism shape with an edge length of approximately 65 Å and a thickness of approximately 35 Å (Fig. 2). It consists of an α and a β domain, which are separated by the heme and by an extended loop of 28 residues (362 to 389) with two 3_{10} helices. Residues 329 to 361 along with 70 NH₂-terminal residues form the β domain, which consists of two β sheets, surrounded by three α helices and one 3_{10} helix. The two-stranded sheet 2 is folded against the five-stranded sheet 1, forming a barrel (Fig. 2). Residues 72 to 325 and 390 to 457 form the α domain. The central feature of the α domain is a right-handed four- α -helix bundle, in which the helices D, I, and L are parallel to each other and anti-parallel to helix E, unlike a classical four- α -helix bundle (22). The helix bundle is bordered at the top by a cluster of five α helices and three 3_{10} helices and at the bottom by three other α helices and two β sheets. The α and β domains account for about 70 percent and 22 percent of the structure, respectively.

The heme is embedded between the I and L helices of the α domain, with no part of it directly exposed to the bulk solvent. As is expected for the low-spin form of the heme in the substrate-free enzyme, Fe(III) is hexacoordinated with Cys⁴⁰⁰ and a water molecule as the axial ligands. The distal axial ligand forms a hydrogen bond with another water molecule and with the carbonyl oxygen of Ala²⁶⁴ (Fig. 1).

Substrate binding pocket. The active site heme is accessible through a long hydrophobic channel, 8 to 10 Å in diameter and lined with mostly nonaromatic hydrophobic residues (Fig. 3). We soaked crystals in mother liquor containing arachidonate, one of the substrates of P450BM-3. A difference electron density map calculated with diffraction data from these crystals and native crystals confirmed our assumption that the channel is the substrate binding site. This substrate binding pocket is defined by the sheet 1 and residues 14 to 25

of the β domain, B', and F helices and the sheet 4 of the α domain. Like the substrate binding pockets in the intestinal fatty acid binding protein (23) and the retinol binding protein (24), the pocket in P450BM-3, a fatty acid hydroxylase, also includes extensive β structure.

The open end of the binding pocket,

close to the molecular surface, is flanked by the side chain of Arg⁴⁷ (Fig. 3). This residue is not well defined in either of the two crystallographically independent molecules; the flexibility of Arg⁴⁷ in P450BM-3 may be necessary to catalyze the mono-oxygenation of fatty acids of different lengths. The narrow end of the substrate

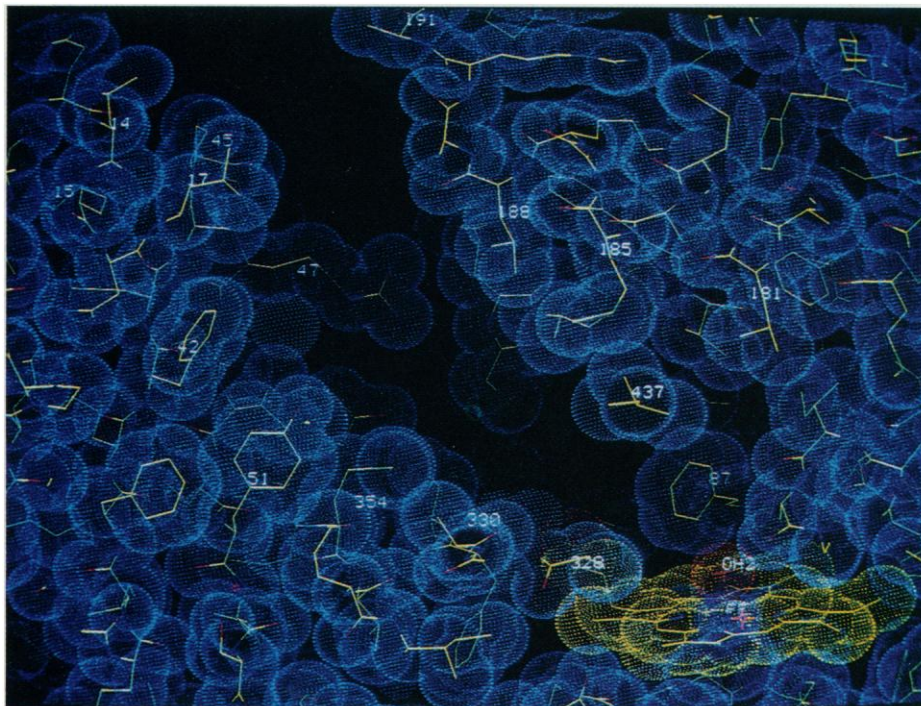


Fig. 3. Van der Waals surface of the substrate binding pocket of molecule 2. This view differs from that in Fig. 2A by about 90° rotation with respect to a horizontal axis. The truncated cone-shaped substrate binding pocket runs diagonally across the figure. The active site heme and the distal axial ligand (OH2) are at the bottom right, with Phe⁸⁷ perpendicular to the heme. The side chain of Arg⁴⁷ protrudes into the pocket. Phe⁴², Tyr⁵¹, Leu¹⁸¹, Met¹⁸⁵, Leu¹⁸⁸, Ala³²⁸, Ala³³⁰, and Met³⁵⁴ line the hydrophobic pocket. Of interest is the close van der Waals interaction between Met¹⁸⁵ and Leu⁴³⁷. Solvent exposed hydrophobic residues (Leu¹⁴, Leu¹⁷, Pro⁴⁵, and Ala¹⁹¹) define the substrate docking region.

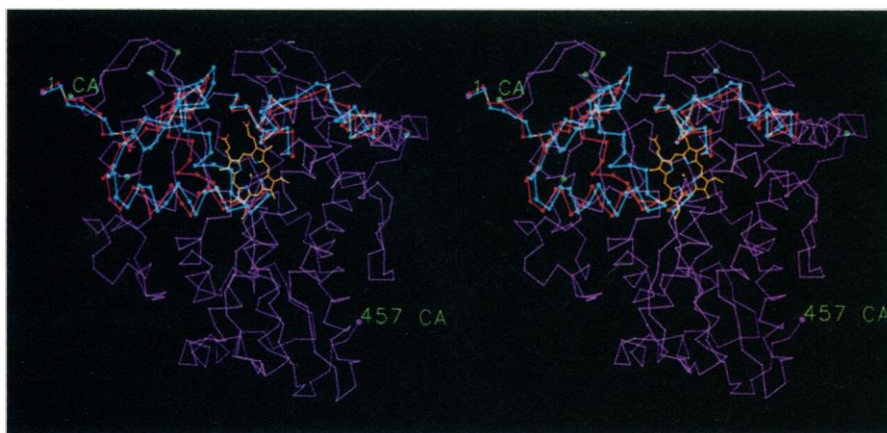


Fig. 4. Stereo C α drawing of the superposition of molecules 1 and 2, viewed as in Fig. 2A. C α atoms of molecule 1 that come within twice the rms value (0.66 Å) of the corresponding atoms in molecule 2 are shown in purple. Those which deviate by more than 0.66 Å due to crystal contacts, common to both molecules, are shown in green. The rest of the C α atoms are shown for molecules 1 (cyan) and 2 (red).

binding pocket is near the active site heme (Fig. 1); Phe⁸⁷ forms close van der Waals interactions with the heme on the distal side, with its phenyl ring almost perpendicular to the porphyrin plane. Hydrophobic interaction of the substrate camphor with aromatic residues was also observed in P450cam (4). The Phe⁸⁷ in P450BM-3 could be important for sequestering the ω -end of a fatty acid, which is not hydroxylated by the enzyme.

The side chains of Met¹⁸⁵ and Leu⁴³⁷ are in close van der Waals contact, stabilizing the packing of sheet 4 against the F helix. Met¹⁸⁵ of P450BM-3 corresponds to Thr¹⁸⁵ of P450cam which belongs to a flexible loop and is involved in substrate interaction (25). Mutation of the corresponding Phe²⁰⁹ to Leu in the mouse microsomal P450coh altered the substrate specificity from coumarin to testosterone (26).

Part of the hydrophobic channel is occupied by residual electron density in both the molecules in the crystal; this density is more pronounced in molecule 2, particularly around residues 15 to 20. A difference-Fourier map of the thimerosal derivative, which was prepared in the absence of dithiothreitol (DTT), shows a substrate binding pocket free of extraneous electron density. Also, DTT inhibits substrate binding to P450BM-3 in solution (27). These results suggest that the residual electron density is due to DTT, a large excess (15 mM) of which was used for crystallization (14). DTT also inhibits substrate binding to P450cam (28) and occupies the active site of the enzyme in crystals grown in its presence (25).

At the entrance of the substrate binding pocket, an exposed hydrophobic patch is formed by the side chains of Phe¹¹, Leu¹⁴, Leu¹⁷, Pro¹⁸, Pro⁴⁵, and Ala¹⁹¹ (Fig. 3). These hydrophobic residues may be important for initial docking of a lipophilic substrate since they are solvent-exposed, mobile, and located adjacent to the binding pocket. Two lysines in this region (Lys⁹ and Lys¹⁵) are protected from trypsin cleavage in the presence of myristate (9). Whereas this region probably does not participate in productive substrate binding, nonspecific binding of a substrate to this hydrophobic patch could nevertheless prevent access of the protease to the lysines.

Conformational heterogeneity and substrate binding. The two molecules in the asymmetric unit of the crystal are related by a rotation of 159.0° around an axis that coincides with the crystallographic *a* axis, and a translation of ~25 Å along this axis. The 457 C α atoms of the two molecules superimpose with an rms deviation of 0.77 Å, significantly higher than the estimated coordinate error. Large differences are observed in the conformation of the two

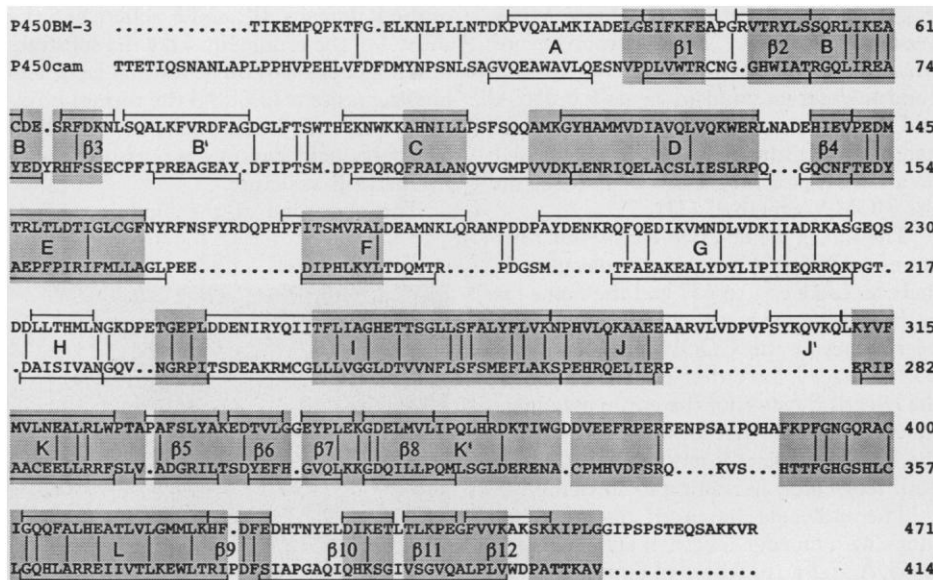


Fig. 5. Sequence alignment of P450BM-3 and P450cam based on their tertiary structures. The two structures were superimposed when the program O is used (18). Residues whose C α atoms come within 2.0 Å are shaded. The secondary structural elements are indicated by a solid line above and below the sequences. The α helices A, B', F, G, K, and J are longer in P450BM-3 compared to those in P450cam, whereas the helices B, C, E, and L are shorter. P450BM-3 has two extra helices (J' and K'). Identical residues are shown by vertical lines between the sequences.

molecules around the substrate binding pocket. As a result, the binding pocket in molecule 2 is in a more open conformation than that in molecule 1 (Fig. 4). Consistent with this, the residual electron density in the pocket is more pronounced in molecule 2. The differences can be described as independent rotations of the β domain by ~5.0° and of the F-G helical region by ~4.6°, relative to the main body of the enzyme. Excluding the β domain and the F-G region, the rms deviation is 0.3 Å, which is in the range of values reported for other proteins (29).

The regions that differ most between the two molecules (rms deviation 1.8 Å) include the residues 1 to 49, 71 to 77 (B' helix), 186 to 208 (F-G region), and 435 to 436 (sheet 4). The conformational flexibility of the NH₂-terminal region (1 to 49), which includes the A helix and the strands β 1-1 and β 1-2, is also expressed in its high B factors. The average B factor of the segment 5 to 24 in molecule 1 is 53 Å², twice that of molecule 2. The decreased flexibility and the more open conformation of the NH₂-terminal region of molecule 2 arise as a result of strong intermolecular interactions in the crystal lattice. The major factors that help stabilize this region in molecule 2 include (i) two ion pairs (ii) Π -electron interactions between three aromatic residues, and (iii) contacts involving several backbone and side chain atoms of residues 5 to 24. The carboxylate of Glu⁴³⁵ interacts with the positive end of the A helix dipole and accounts for the displacement of Glu⁴³⁵ and Thr⁴³⁶ in molecule 2.

In contrast, differences in the conformation of B' helix and the F-G region can be attributed to crystal contacts of these regions in only molecule 1. Most likely, the substrate binding pocket of P450BM-3 is highly dynamic and can adopt many conformations in solution.

P450BM-3 and P450cam represent the two classes of P450 and the size and structure of their preferred substrates differ significantly. The amino acid sequence identity between them is only 16 percent (Fig. 5). The rms deviation for 245 C α atoms is 2.0 Å between the two P450 structures. While the overall folding and the percentages of α helices (~50 percent) and β sheet (~15 percent) are very similar in the two proteins, their relative arrangements differ substantially. Helices A, B', C, G, and H are displaced significantly between the two structures. For example, the helix axis of B', residues of which participate in substrate binding, is rotated by ~100° between the two structures. Except for two β strands, corresponding to β 2 in P450cam (4), the rest of the β strands are present in both the enzymes. The COOH-terminal portion of the I helix (268 to 282), the L helix (402 to 419), and the loop containing the cysteine that coordinates the heme (390 to 400) are structurally conserved. All P450s also exhibit high amino acid sequence similarity in these regions.

P450BM-3 has four major insertions relative to P450cam (Fig. 5). The first insertion consists of ten residues with a 3₁₀

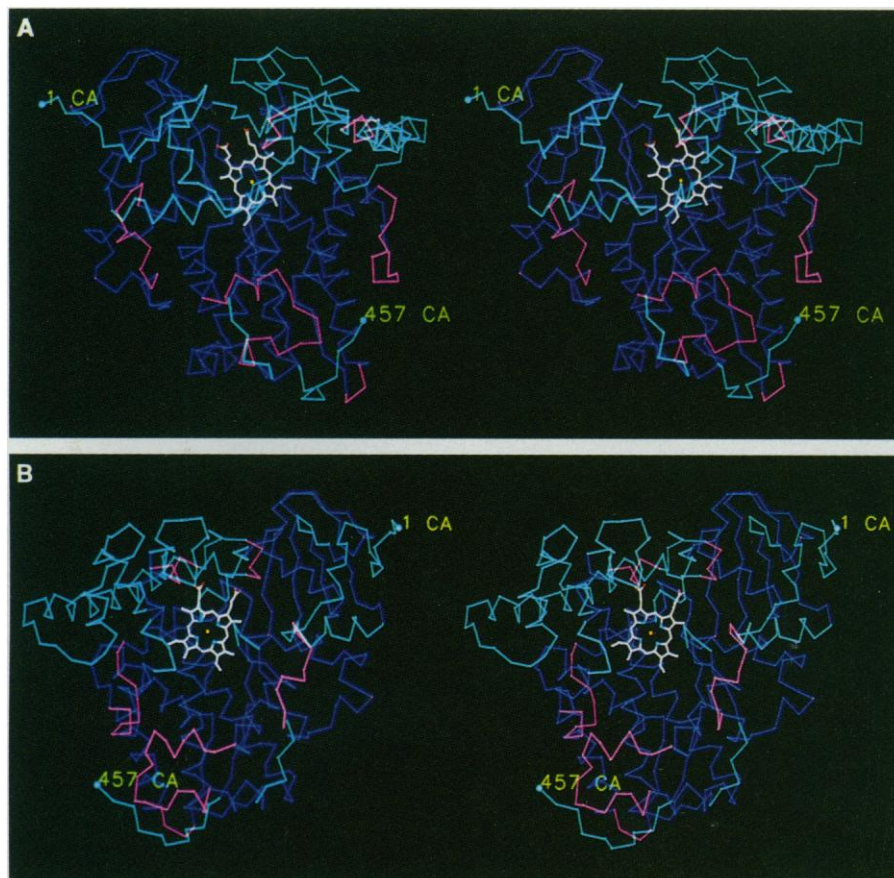


Fig. 6. Comparison of the tertiary structures of P450BM-3 (molecule 2) and P450cam. The C α atoms of the two molecules were superimposed as described in the legend to Fig. 5. The C α atoms of P450BM-3 which superimpose within 2.0 Å of the corresponding atoms in P450cam are shown in blue. Those which deviate by more than 2.0 Å are shown in cyan while purple represents the insertions in P450BM-3. (A) View down the substrate access channel. (B) View from the redox partner binding site.

helix, flanked on either side by loops that connect it to the E and F helices. The second consists of 11 residues, which extend both the F and G helices. The two protein structures differ significantly around this insertion (Fig. 6A). Differences are also seen in the NH₂-terminal part (1 to 49), the loop between B' and C helices, B', E, F, G, and H helices, and the sheet 4. Many of these structural differences occur around the substrate binding pocket and could thus confer different substrate specificities.

The longest insertion (17 residues) is between the J and K helices (Fig. 5). This results in the elongation of the J helix by two turns and the formation of a new helix (J'). The last insertion, seven residues long, is centered around Ile³⁸⁵ and consists of two 3₁₀ helices. Absence of major deletions in P450BM-3 with respect to P450cam, one of the smallest cytochromes P450, suggests that P450cam fulfills the minimal structural requirements that characterize a P450.

The reducing equivalents required for catalysis are provided by a reductase covalently attached to the P450 domain in

P450BM-3. A similar electron transfer process occurs in the microsomal redox system where the P450 and the reductase are separate. The presence of KCl inhibits monooxygenation of fatty acids by the reconstituted system containing the two recombinant domains of P450BM-3, indicating that the interaction between the redox partners is primarily electrostatic (30). Site-directed mutagenesis has also suggested a role for positively charged residues on microsomal P450's for interaction with the reductase (31).

The structure of the hemoprotein domain defines a putative docking site, a rectangular depression of 35 by 17 by 10 Å for the redox partner on the proximal side of the heme (Fig. 6B). The outer edge is formed by the α helices B, C, D, J', and K and four 3₁₀ helices (b, c, e, and f). A cluster of positively charged residues protrude from this region and could aid in the initial docking of the redox partner. Modeling studies on P450cam have also suggested a similar surface for binding the redox partner (32).

The inner portion of the docking site is formed primarily by the segment 390 to 408. Several apolar residues in this region, together with those from the outer edge, define an exposed hydrophobic floor of the depression. The exposed hydrophobic region, on the molecular surface, could also participate in specific interactions with the redox partner as has been proposed for the complex between cytochrome c peroxidase and cytochrome c (33).

Other features of the proposed redox partner docking site include the preponderance of neutral amino acids, such as glutamines, the presence of four 3₁₀ helices around the depression, and structural differences between P450BM-3 and P450cam on the outer edge. The J' helix and the 3₁₀ helix f, which are insertions in P450BM-3 with respect to P450cam, define two of the edges of the rectangular depression (Fig. 6B). P450BM-3 is the only known bacterial P450 with these insertions which are characteristic of eukaryotic P450's. Structural changes are also observed in the C-D helical region of P450BM-3. The C helix is followed by D helix in P450cam, but it is shortened by nine residues in P450BM-3 and is replaced by two 3₁₀ helices (b and c) at the COOH-terminal end.

The I helix and its functional significance. A prominent feature of the P450 structures is the 50 Å long I helix. The hydrogen bonding pattern is disrupted in the region Ile²⁶³ to Thr²⁶⁹ of the I helix, the region that flanks the distal side of the heme. Three hydrogen bonds from the carbonyl oxygens of Ile²⁶³, Ala²⁶⁴, and Gly²⁶⁵ to the amide nitrogens of Glu²⁶⁷, Thr²⁶⁸, and Thr²⁶⁹, respectively, are absent because of the water molecule 1164 (Fig. 1). The coordination environment around this water molecule resembles a distorted tetrahedron, with the amide nitrogens of Glu²⁶⁷ and Thr²⁶⁸ as proton donors and the carbonyl oxygens of Ile²⁶³ and Ala²⁶⁴ as acceptors. In addition, the O γ of Thr²⁶⁸ and Thr²⁶⁹ form hydrogen bonds with the carbonyl oxygens of Ala²⁶⁴ and Gly²⁶⁵. The helix is bent and stretched out in this region, forming a large groove, adjacent to the axial ligand.

P450cam also contains a groove, comparable in size to that in P450BM-3, in the I helix. However, it is located in the next turn of the I helix, away from the heme in P450cam, and it also contains a water molecule. A least-squares superposition of the two structures in this region (263 to 271 of P450BM-3) results in an rms deviation of 1.0 Å for the 36 backbone atoms, a value unusually large for two helical segments. Modeling studies indicate that dioxygen bound to the iron does not protrude into the groove of either of the P450 structures.

Hence, it is unlikely that the groove is required for oxygen binding.

One of the critical steps in the P450 reaction cycle is the protonation of dioxygen bound to the reduced heme. Several models have been proposed to account for the source of protons required for oxygen activation (34, 35). An internal solvent channel consisting of three water molecules between Thr²⁵² and Glu³⁶⁶ of the L helix in P450cam was proposed to be the source of protons (34). No such solvent channel exists in P450BM-3 even though both these residues are conserved (Thr²⁶⁸ and Glu⁴⁰⁹).

The groove in the I helix of P450BM-3 is flanked by two charged residues, His²⁶⁶ and Glu²⁶⁷. In addition to the conserved threonine at position 268, most of the cytochromes P450 have a serine or threonine at 269 and an acidic residue at 267. Sligar and co-workers have proposed that this acidic residue plays a crucial role in proton transfer to the threonine and gets protonated anew by a charge relay mechanism (35). While in P450cam, the acidic residue forms salt bridges with two basic residues from the F helix (34), no such interactions are observed in P450BM-3. The F-G helix pair in P450BM-3 is translated laterally, thereby partially exposing the heme as well as His²⁶⁶ and Glu²⁶⁷ to the solvent.

It is believed that the conserved threonine (Thr²⁶⁸) donates a proton to iron-bound oxygen during catalysis. The water molecule located in the groove of the I helix in P450BM-3 could transfer protons to O_γ of Thr²⁶⁸. The water molecule, in turn, could be protonated by Glu²⁶⁷, which is solvent-exposed in P450BM-3. Thus, the proton transfer pathway to molecular oxygen in P450BM-3 involves three essential

components: the ordered water molecule in the groove of the I helix, the conserved threonine, and the acidic residue that precedes the threonine.

Even though both P450BM-3 and P450cam are bacterial enzymes, they differ significantly in their tertiary structures, substrate specificities, and redox partner preferences. Unlike other bacterial P450's, P450BM-3 has a high amino acid sequence identity and bears close functional resemblances to the microsomal P450's. The structural features of P450BM-3, hence, may represent that of a class II P450 and could be useful for a better understanding of the structure-function relation of microsomal P450's.

REFERENCES AND NOTES

1. T. D. Porter and M. J. Coon, *J. Biol. Chem.* **266**, 13469 (1991); F. J. Gonzalez, *Pharmacol. Rev.* **40**, 243 (1988); A. B. Okey, *Pharmacol. Ther.* **45**, 241 (1990).
2. D. R. Nelson *et al.*, *DNA Cell Biol.* **12**, 1 (1993).
3. F. P. Guengerich, *J. Biol. Chem.* **266**, 10019 (1991); P. R. Ortiz de Montellano, *Cytochrome P-450: Structure, Mechanism, and Biochemistry* (Plenum, New York, 1986), pp. 217–257.
4. T. L. Poulos, B. C. Finzel, A. J. Howard, *J. Mol. Biol.* **195**, 687 (1987).
5. I. C. Gunsalus, J. R. Meeks, J. D. Lipscomb, P. G. Debrunner, E. Munch, *Molecular Mechanisms of Oxygen Activation* (Academic Press, New York, 1974).
6. T. L. Poulos and R. Raag, *FASEB J.* **6**, 674 (1992).
7. T. L. Poulos, *Methods Enzymol.* **206**, 11 (1992).
8. A. J. Fulco, *Annu. Rev. Pharmacol. Toxicol.* **31**, 177 (1991).
9. L. O. Narhi and A. J. Fulco, *J. Biol. Chem.* **262**, 6683 (1987).
10. T. Oster, S. S. Boddupalli, J. A. Peterson, *ibid.* **266**, 22718 (1991); H. Y. Li, K. Darwish, T. L. Poulos, *ibid.*, p. 11909.
11. S. S. Boddupalli, T. Oster, R. W. Estabrook, J. A. Peterson, *ibid.* **267**, 10375 (1992).
12. T. D. Porter, *Trends Biochem. Sci.* **16**, 154 (1991).
13. R. T. Ruettinger, L. Wen, A. J. Fulco, *J. Biol. Chem.* **264**, 10987 (1989).
14. S. S. Boddupalli *et al.*, *Proc. Natl. Acad. Sci. U.S.A.* **89**, 5567 (1992).
15. T. A. Jones, *J. Appl. Crystallogr.* **11**, 268 (1978).
16. ———, J.-Y. Zou, S. W. Cowan, M. Kjeldgaard, *Acta Crystallogr. A* **47**, 110 (1991).
17. W. Steigemann, paper presented at the American Crystallographic Association Annual Meeting, Toledo, OH, July 1992.
18. We thank Dr. F. M. D. Vellieux for the DEMON program for density averaging.
19. A. T. Brünger, J. Kuriyan, M. Karplus, *Science* **235**, 458 (1987); A. T. Brünger, *Nature* **355**, 472 (1992).
20. V. Luzzati, *Acta Crystallogr.* **5**, 802 (1952).
21. R. J. Read, *ibid.* **A42**, 140 (1986).
22. S. C. Presnell and F. E. Cohen, *Proc. Natl. Acad. Sci. U.S.A.* **86**, 6592 (1989).
23. J. C. Sacchettini, G. Scapin, D. Gopaul, J. I. Gordon, *J. Biol. Chem.* **267**, 23534 (1992).
24. M. E. Newcomer *et al.*, *EMBO J.* **3**, 1451 (1984).
25. T. L. Poulos, B. C. Finzel, A. J. Howard, *Biochemistry* **25**, 5314 (1986).
26. R. Lindberg and M. Negishi, *Nature* **339**, 632 (1989).
27. S. S. Boddupalli, unpublished material.
28. M. Sono, L. A. Anderson, J. H. Dawson, *J. Biol. Chem.* **257**, 8308 (1982).
29. C. Chothia and A. M. Lesk, *EMBO J.* **5**, 823 (1986).
30. J. A. Peterson, T. Oster, S. S. Boddupalli, in *Cytochrome P450: Biochemistry and Biophysics*, A. I. Archakov and G. I. Bachmanova, Eds. (INCO-TNC Press, Moscow, 1992), pp. 708–715.
31. H. Furuya *et al.*, *Biochemistry* **28**, 6848 (1989).
32. P. S. Stayton, T. L. Poulos, S. G. Sligar, *ibid.*, p. 8201.
33. H. Pelletier and J. Kraut, *Science* **258**, 1748 (1992).
34. R. Raag, S. A. Martinis, S. G. Sligar, T. L. Poulos, *Biochemistry* **30**, 11420 (1991).
35. N. C. Gerber and S. G. Sligar, *J. Am. Chem. Soc.* **114**, 8742 (1992).
36. Coordinates of the hemoprotein domain of P450BM-3 have been deposited in the Brookhaven Data Bank (entry code 1HPD).
37. We thank D. Diggs for help with various programs for structure analysis, K. Fischer-Lindahl and D. Corey for review and suggestions, and D. Staber for assistance in the preparation of the manuscript. Computing resources for this work were provided by The University of Texas System Center for High Performance Computing. Supported in part by NIH grant GM43479 (to J.A.P.) and the Howard Hughes Medical Institute.

1 March 1993; accepted 17 June 1993